Journal of Materials Chemistry C

Accepted Manuscript

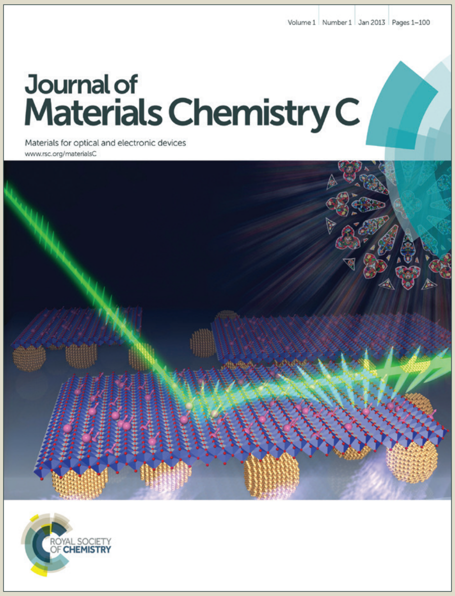

ROYAL SOCIETY OF CHEMISTRY

www.rsc.org/materialsC

Cite this: DOI: 10.1039/c0xx00000x

www.rsc.org/xxxxxx

ARTICLE TYPE

Heating-rate dependence of spin-crossover hysteresis observed in an iron(II) complex having tris(2-pyridyl)methanol[†]

Masaru Yamasaki[a] **and Takayuki Ishida**[*,a]

Received (in XXX, XXX) Xth XXXXXXXXX 20XX, Accepted Xth XXXXXXXXX 20XX

DOI: 10.1039/b000000x

$Me_4N[Fe(py_3COH)(NCS)_3](H_2O)$ showed an abrupt spin-crossover with thermal hysteresis, and temperature-scan rate dependence was recorded on heating with 10 – 0.02 K min^{-1}. At the slowest scan the product of magnetic susceptibility and temperature once increased at 246 K, turned to decrease around 250 K and finally increased again to reach the high-spin state around 280 K. A polymorphic spin-crossover model is plausible.

Spin-crossover (SCO) behaviour is a reversible transition between low-spin (LS) and high-spin (HS) states by external stimuli like heat, light, pressure and so on.[1-3] For development of multi-functional materials involving thermo- and photo-chromisms and magnetisms, bistability displaying thermal hysteresis is a key factor.[1-3] SCO thermal hysteresis is sometimes found to accompany a structural phase transition.[4] Intermolecular interactions such as hydrogen-bonding and π–π stacking are important for SCO cooperativity[5] as well as bulk transition.

The tripodal compound py_4C (py = 2-pyridyl) has been developed as a LIESST ligand (LIESST stands for light-induced excited spin-state trapping),[6] and another tripod py_3COH works as a hysteretic-SCO and LIESST ligand.[7] These tris(2-pyridyl)methane derivatives (py_3CR) are promising for SCO-oriented crystal engineering, because an approximate three-fold symmetry is just suitable for two-dimensional crystalline supramolecular architecture and cooperativity. It should be noted that py_3CR ligands are neutral, and accordingly $[Fe(py_3CR)(NCS)_3]^-$ units are negatively charged. Anionic SCO building blocks are relatively rare.[6-8] Various counter cations are available to explore novel SCO materials.

Very recently, we have developed $Me_4N[Fe(py_3COH)(NCS)_3](PrOH)_{0.5}(H_2O)_2$ (**1**), and **1** was annealed by heating at 100-120 °C for 50 min, to give $Me_4N[Fe(py_3COH)(NCS)_3](H_2O)$ (**1'**).[7] The composition was determined by means of elemental analysis. We found that **1** is very efflorescent, and the specimen of **1'** became fine powder. To avoid such efflorescence we selected a hydrophobic tripod py_3CMe[9] and counter cations with longer alkyl groups and now successfully prepared an unsolvated analogue $Bu_4N[Fe(py_3CMe)(NCS)_3]$† (**2**). The magnetic properties of **2** will be noted later, but at this stage we have to stress that py_3CR derivatives are robust SCO ligands.

The X-ray crystallographic analysis on **2**‡ clarified that **1** and **2** were isomorphous. The asymmetric unit of the crystal of **2** involves $[Fe(py_3CMe)(NCS)_3]^-$ and Bu_4N^+ each, and the anionic moiety shows an approximate C_{3v} symmetry. Apparently π–π interaction is characterized between the py rings in an intermolecular fashion, thus giving a pseudo-trigonal lattice parallel to the crystallographic *ab* plane (Figure 1). The py···py separation was evaluated with the distance between the centres of the py rings. In **2** the distances are 3.74, 3.70 and 3.71 Å.

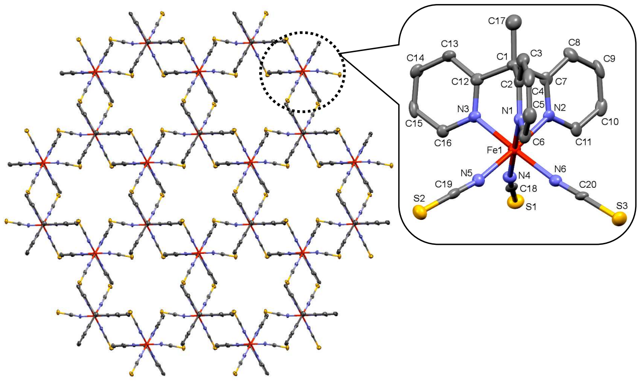

Figure 1. Two-dimensional molecular arrangement of the $[Fe(py_3CMe)(NCS)_3]^-$ moiety in **2**. Hydrogen atoms are omitted for the sake of clarity. The thermal ellipsoids are drawn at the 50% level.

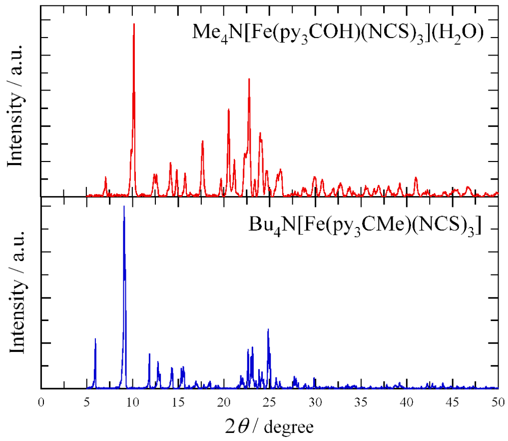

Figure 2. Powder XRD profiles for **1'** (top) and **2** (bottom), measured by using Cu Kα irradiation.

The characterization of **2** helps us to understand the structure of powdery **1'**. The powder XRD profiles of **1'** and **2** are similar to each other (Figure 2), especially in 2θ = 5 – 15°, suggesting that they have an isomorphous layered structure. The diffractions assigned to (0 0 1) and (0 0 2) were found at $2\theta = 7.10$ and 14.20° for **1'** and 5.94 and 11.85° for **2**. The layer distances (d) are 12.5 and 14.9 Å, respectively. This result also clarifies that the removal of the lattice solvent molecules in **1** shrank the unit cell, as indicated by $d = 13.414(3)$ Å for **1**[7] and $d = 12.5$ Å for **1'**.

The magnetic susceptibility of powdery **1'** was measured on a Quantum Design SQUID magnetometer (MPMS-XL7) in a temperature range of 1.8 – 400 K. Figure 3 summarizes the results on the heating-rate dependence of SCO of **1'**. At a relatively fast scan rate (10 K min^{-1} for example), an abrupt SCO was observed at $T_{1/2}\downarrow = 224$ K and $T_{1/2}\uparrow = 246$ K. The hysteresis is reproduced in the differential scanning calorimeter analysis, and the width was determined to be 22 K. Intermolecular interaction parameter Γ was evaluated according to the Slichter-Drickamer model.[10] Simulation gave $\Gamma = 4.9$ kJ mol^{-1}, which is larger than $2RT_{\text{SCO}} = 3.91$ kJ mol^{-1}. This finding indicates that the cooperativity is substantial.

Most interestingly, at slower scan rates, the $\chi_{\text{m}}T$ values at the HS state region largely decreased, and the measurements with slower rates showed more drastic decreases. At 250 K on the way of heating, the $\chi_{\text{m}}T$ values varied as ca. 3, 2 and 1 cm^3 K mol^{-1} when measured with the scan rates of 1, 0.1 and 0.02 K min^{-1}, respectively. Finally we recorded a total hysteresis width of 60 K at a rate of 0.02 K min^{-1}. The final $\chi_{\text{m}}T$ levels were unchanged (3.7 cm^3 K mol^{-1} at 300 K). On the other hand, no anomaly of the $\chi_{\text{m}}T$ profile was recorded on cooling even at the slowest run.

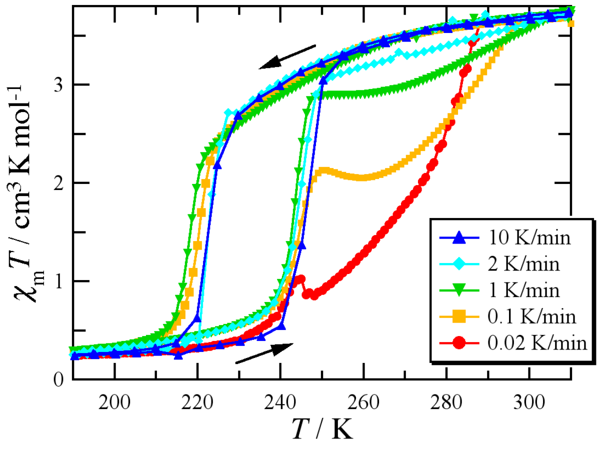

Figure 3. Temperature scan rate dependence of the SCO of **1'**. The applied field was 0.5 T.

There have been a few reports on temperature-scan-rate dependence of T_{SCO}.[11,12] In that case, a fast scan elevated $T_{\text{SCO}}\uparrow$ on heating and expanded thermal hysteresis in a cycle. It was explained in terms of the thermally activated mechanism.[12] In sharp contrast, the present study on **1'** showed a reverse trend, as the slower scans gave an apparent higher $T_{\text{SCO}}\uparrow$ and wider hysteresis. A simple activation model does not hold for **1'**.

Obviously the present SCO behaviour on **1'** (Figure 3) involves double SCO transitions, an original one at 246 K and a new one around 280 K. Accordingly, we have to introduce another LS state, in particular to interpret the $\chi_{\text{m}}T$ drop region, just like "reverse SCO."[13] A clue may reside in the coexistence of a metastable state or polymorph.[3] If we think that two solid states for crystalline **1'** are present, this phenomenon will be understood, as depicted in Figure 4. Here, to simplify a model, hysteresis width is disregarded; the transition temperatures are located as for heating process. Phases α and β have their LS and HS phases (i.e., LSα, HSα, LSβ and HSβ phases). The slow heating process clarified the presence of hidden LSβ, but the cooling process did not guarantee the presence of another HS state. Therefore, three phases are enough to describe the present SCO phenomenon. It is natural that the HSα line successively crosses with the LSα and LSβ lines, which correspond to two SCO points ($T_{\text{SCO}}(\alpha) < T_{\text{SCO}}(\beta)$). We can assign $T_{\text{SCO}}(\alpha)\uparrow = 246$ K and $T_{\text{SCO}}(\beta)\uparrow = 280$ K from the experimental results (Figure 3).

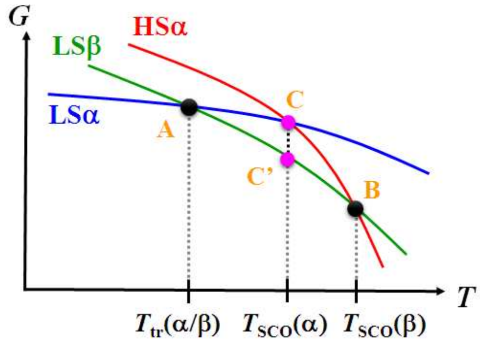

Figure 4. A schematic drawing of Gibbs free energy diagram for **1'**, which describes a mechanism for the heating-rate dependence of SCO.

The transition from C to C' (Figure 4) accompanies an appreciable activation energy, because two transitions, the (structural) phase transition between α and β phases and spin transition between HS and LS states, take place at the same time. The origin of the former is unclear at present because of the lack of detailed structural information, but it may be related with molecular or substituent configuration in the solid state. Hysteretic behaviour requires an appreciable latent heat upon first-order transition, and accordingly this must be a structural phase transition.

Transition probability of branching C → C' and C → B is crucial. When the temperature scan is fast, most iron(II) ions move along LSα → C → HSα → B → HSα. Level-crossing A is not observed and LSβ does not appear, possibly because the thermal energy at $T_{\text{tr}}(\alpha/\beta)$ is insufficient to surpass the activation energy barrier. When the scan is slow, a partial population would undergo a relaxation, like LSα → C → C' → LSβ → B → HSα.

From a closer look at the final transition around 280 – 290 K, a faster temperature scan brings T_{SCO} to a higher temperature. This finding supports the presence of the activation energy at $T_{\text{SCO}}(\beta)$. It would be normal if we suppose that level-crossing B includes the structural α/β-phase transition.

If we cool **1'**, the iron(II) spin state is supposed to trace a simple way like HSα → C → LSα. Crossing B is completely buried, because this transition has intrinsic hysteresis as described above. We can imagine that $T_{\text{SCO}}(\beta)\downarrow$ is lower than $T_{\text{SCO}}(\beta)\uparrow$ and further that $T_{\text{SCO}}(\beta)\downarrow$ might also be located lower than $T_{\text{SCO}}(\alpha)\uparrow$ by accident. The Gibbs free energy diagram drawn in Figure 4 is plausible to describe qualitatively the total SCO observation on **1'**.

Real and co-workers reported a similar SCO system,[14] which has also been explained in terms of double SCO. Polymorphs are often realized by introduction of long alkyl chains.[3,13] Real's compound possesses three butyl groups providing a conformational isomerism. Our compound has differentiated the source of polymorph; **1'** has only methyl groups. Hydrogen bonds among py$_3$COH and H_2O may contribute to polymorphism. However, unfortunately, this argument is speculative because the crystal structure of **1'** has not yet been determined.

Compound **2** showed a gradual SCO around 330 K but no hysteresis or no dynamics like **1'**. One may ask why the two compounds behaved so differently. It is because π- π interaction between the py rings is weak in **2**, though they are located in a face-to-face manner. The separations of the py rings are 3.71 Å for **2** and 3.66 Å for **1**[7] on the average. They are longer than the π–π contact distance (3.5 Å).[15] It is reasonable that both **1** and **2** showed only gradual SCO. The crystal packing became tight after the removal of the solvent molecules and cooperative interaction would be enhanced.[16] In **1'** the cell shrinkage is evidenced by the XRD study. Actually, the layer separation was shortened by 7% on removal of the solvent. The *a* and *b* axis lengths would be concomitantly shortened, as expected from the location of the lattice solvent molecules in the crystal of **1**.[7]

In conclusion, the heating-rate dependence of SCO was recorded on **1'**, which includes an apparent "reverse SCO" in a limited temperature region. The slower heating scans gave the higher $T_{\mathrm{SCO}}\uparrow$ and wider hysteresis. A plausible mechanism is proposed, where the structural phase transition in a polymorphic solid is coupled and/or interfered with the SCO transitions of two phases.

This work was partly supported by KAKENHI (Grant Numbers JSPS/15H03793). We are grateful to Prof. Yoshio Kobayashi and Mr. Daiki Natori for kind assistance in experiments.

Notes and references

[a] *Department of Engineering Science, The University of Electro-Communications, Chofu, Tokyo 182-8585, Japan. Fax: 81 42 443 5501; Tel: 81 42 443 5501; E-mail: ishi@pc.uec.ac.jp*

† Compound **2** was prepared from py$_3$CMe[9] (28 mg; 0.1 mmol), Bu$_4$NBr (101 mg; 0.3 mmol), LiSCN·nH$_2$O (60% assay) (117 mg; 1.1 mmol) and FeCl$_2$·4H$_2$O (70 mg; 0.3 mmol) in methanol (14 mL) in the presence of L-ascorbic acid (8 mg) as an antioxidant. Reddish black crystals were precipitated and collected on a filter. The yield was 28 mg (37%). M.p. 219-222˚C. IR (neat ATR): 462, 488, 514, 565, 636, 650, 735, 766, 794, 847, 877, 919, 1031, 1052, 1109, 1160, 1245, 1303, 1386, 1437, 1459, 1562, 1591, 2068, 2098, 2869, 2928, 2954, 2993, 3086 cm^{-1}. Anal. Calcd.: C, 58.92, H, 7.01, N, 13.36, S, 13.11% for $C_{36}H_{51}FeN_7S_3$. Found: C, 59.22, H, 7.29, N, 13.52, S, 13.24%.

‡ X-Ray diffraction data of **2** were collected on a Rigaku Mercury CCD diffractometer with graphite monochromated MoKα radiation (λ = 0.71073 Å). The structures were directly solved by a heavy-atom method and expanded using Fourier techniques in the CRYSTALSTRUCTURE program package.[17] Selected crystallographic data are: $C_{36}H_{51}FeN_7S_3$, FW 733.87, triclinic, *P*-1, a = 12.173(6), b = 12.280(5), c = 16.068(8) Å, α = 69.861(18), β = 69.023(18), γ = 60.628(15)°, V = 1912.0(15) Å^3, Z = 2, d_{calc} = 1.275 g cm^{-3}, μ(MoKα) = 0.593 mm^{-1}, $R(F)$ ($I > 2\sigma(I)$) = 0.0795, $R_{\mathrm{W}}(F^2)$ (all data) = 0.0928, and T = 100 K for 7807 unique reflections. The Fe-N bond lengths varied in 1.942(5) – 1.958(5) Å, suggesting that **2** is in a LS phase at 100 K. CCDC 1053453. These data can be obtained free of charge via http://www.ccdc.cam.ac.uk/conts/retrieving.html.

1 P. Gütlich and H. A. Goodwin Eds. *Spin Crossover in Transition Metal Compounds I, II, and III*; Springer-Verlag: Berlin, 2004; P. Gütlich, A. Hauser and H. Spiering, *Angew. Chem., Int. Ed. Engl.*, 1994, **33**, 2024.

2 M. A. Halcrow, Ed. *Spin-crossover Materials: Properties and Applications*; John Wiley & Sons: Chichester, UK, 2013; M. A. Halcrow, *Polyhedron*, 2007, **26**, 3523; M. A. Halcrow, *Chem. Soc. Rev*., 2011, **40**, 4119; J. A. Real, A. B. Gaspar and M. C. Münoz, *Dalton Trans.*, 2005 2062.

3 Y. Oso, D. Kanatsuki, S. Saito, T. Nogami and T. Ishida, *Chem. Lett.*, 2008, **37**, 760; Y. Oso and T. Ishida, *Chem. Lett.*, 2009, **38**, 604.

4 S. Lakhloufi, P. Guionneau, M. Lemee-Cailleau, P. Rosa and J. Letard, *Phys. Rev. B.* 2010, **82**, 132104 ; Y. Miyazaki, T. Nakamoto, S. Ikeuchi, A. Inaba, M. Sorai, T. Tojo, T. Atake, G. S. Matouzenko, S. Zein and S. A. Borshch, *J. Phys. Chem. B*. 2007, **111**, 12508.

5 J. A. Real, A. B. Gaspar, V. Niel and M. C. Münoz, *Coord. Chem. Rev.*, 2003, **236**, 121.

6 N. Hirosawa, Y. Oso and T. Ishida, *Chem. Lett.*, 2012, **41**, 716.

7 M. Yamasaki and T. Ishida, *Polyhedron*, 2015, **85**, 795.

8 M. Yamada, M. Ooidemizu, Y. Ikuta, S. Osa, N. Matsumoto, S. Iijima, M. Kojima, F. Dahan and J.-P. Tuchagues, *Inorg. Chem.*, 2003, **42**, 8406; Y. Sunatsuki, H. Ohta, M. Kojima, Y. Ikuta, Y. Goto, N. Matsumoto, S. Iijima, H. Akashi, S. Kaizaki, F. Dahan and J.-P. Tuchagues, *Inorg. Chem.*, 2004, **43**, 4151; S. Schlamp, J. Schulten, R. Betz, T. Bauch, A. V. Mudring and B. Weber, *Z. Anorg. Allg. Chem.*, 2012, 1093-1102.

9 A. Maleckis, J. W. Kampf and M. S. Sanford, *J. Am. Chem. Soc.*, 2013, **135**, 6618; E. A. Ünal, D. Wiedemann, J. Seiffert, J. P. Boyd and A. Grohmann, *Tetrahedron Lett.*, 2012**, 53**, 54.

10 C. P. Slichter and H. G. Drickamer, *J. Chem. Phys.*, 1972, **56**, 2142.

11 R. Kulmaczewski, J. Olguín, J. A. Kitchen, H. L. C. Feltham, G. N. L. Jameson, J. L. Tallon and S. Brooker, *J. Am. Chem. Soc*., 2014, **136**, 878.

12 O. Roubeau, M. Castro, R. Burriel, J. G. Haasnoot and J. Reedijk, *J. Phys. Chem. B*, 2011, **115**, 3003; F. J. M.-Lara, A. B. Gaspar, D. Aravena, E. Ruiz, M. C. Munoz, M. Ohba, R. Ohtani, S. Kitagawa and J. A. Real, *Chem. Commun*., 2012, **48**, 4686.

13 S. Hayami, Y. Shigeyoshi, M. Akita, K. Inoue, K. Kato, K. Osaka, M. Takata, R. Kawajiri, T. Mitani and Y. Maeda, *Angew. Chem. Int. Ed.*, 2005, **44**, 4899; S. Hayami, Y. Komatsu, T. Shimizu, H. Komihata and Y. H. Lee, *Coord. Chem. Rev.*, 2011, **255**, 1981; S. Hayami, M. Nakaya, H. Ohmagari, A. S. Alao, M. Nakamura, R. Ohtani, R. Yamaguchi, T. Kuroda-Sowa and J. K. Clegg, *Dalton Trans.*, 2015, doi: 10.1039/C4DT03743J.

14 M. Seredyuk, M. C. Muñoz, M. Castro, T. Romero-Morcillo, A. B. Gaspar and J. A. Real, *Chem. Eur. J.*, 2013, **19**, 6591.

15 A. Bondi, *J. Phys. Chem.*, 1964, **68**, 441.

16 Y. Garcia, P. J. van Koningsbruggen, R. Lapouyade, L. Foumes, L. Rabardel, O. Kahn, V. Ksenofontov, G. Levchenko and P. Gutlich, *Chem. Mater.*, 1998, **10**, 2426; K. B. Duriska, S. M. Neville, B. Moubaraki, J. A. Cashion, G. J. Halder, K. W. Chapman, C. Balde, J. F. Letard, K. S. Murray and C. J. Kepert, *Angew. Chem. Int. Ed.*, 2009, **48**, 2549; W. Zhang, F. Zhao, T. Liu, M. Yuan, Z.-M. Wang and S. Gao, *Inorg. Chem.*, 2007, **46**, 2541; I. Salitros, J. Pavlik, R. Boca, O. Fuhr, C. Rajadurai and M. Ruben, *CrystEngComm*, 2010, **12**, 2361.

17 *CRYSTALSTRUCTURE, version 4.0*, Rigaku/MSC, The Woodlands, TX 77381, USA (2010).

Heating-rate dependence of spin-crossover hysteresis observed in an iron(II) complex having tris(2-pyridyl)methanol

Masaru Yamasaki and Takayuki Ishida*

Department of Engineering Science, The University of Electro-Communications,
Chofu, Tokyo 182-8585, Japan

A Table of Contents Entry.

$Me_4N[Fe(py_3COH)(NCS)_3](H_2O)$ showed an abrupt spin-crossover with thermal hysteresis, and temperature-scan rate dependence was recorded on heating.